Development of lung tissue phantoms for bioluminescent imaging

Durairaj Kumar, Wenxiang Cong, Frank Bohenkamp, Tarun Kakaday, Peter Taft, et al.

Durairaj Kumar, Wenxiang Cong, Frank Bohenkamp, Tarun Kakaday, Peter Taft, Lihong V. Wang, Geoffrey McLennan, Eric A. Hoffman, Ge Wang, "Development of lung tissue phantoms for bioluminescent imaging," Proc. SPIE 5535, Developments in X-Ray Tomography IV, (26 October 2004); doi: 10.1117/12.560530

SPIE.

Event: Optical Science and Technology, the SPIE 49th Annual Meeting, 2004, Denver, Colorado, United States

Development of lung tissue phantoms for bioluminescent imaging

D. Kumar[a], Cong Wenxiang[a], Frank Bohenkamp[a], Tarun Kakaday[c], Peter Taft[c], Lihong V. Wang[d], McLennan Geoffrey[c], Eric A. Hoffman, and *Ge Wang[a, b]
[a]Bioluminescence Tomography Laboratory
[b]CT/Micro-CT Laboratory,
Dept. of Radiology,
[c]Dept. of Internal Medicine
Univ. of Iowa, Iowa, IA, USA 52242
[d]Dept. of Biomedical Engineering, Texas A&M Univ., TX, USA 77843-3120.

ABSTRACT

White nylon material was chosen to make cylindrical tissue phantoms for development of bioluminescence tomography techniques. A low-level light source, delivered through a optic fiber of core diameter 200μm, was placed at different locations on one phantom surface. The light travels through the phantom, reaches the external surface, and is captured by a liquid nitrogen-cooled CCD camera. The scattering, absorption, and anisotropy parameters of the phantom are obtained by matching the measured light transmission profiles to the profiles generated by the TracePro software. The perturbation analysis, with the homogeneous phantoms, demonstrated that the imaging system is sufficiently sensitive to capture intensity change of higher than 0.5nW/cm^2 or a location shift of the light source of more than 200microns. It is observed that the system can distinguish two point light sources with separation of about 2mm. The perturbation analysis is also performed with the heterogeneous phantom. Based on our data, we conclude that there is inherent tomographic information in bioluminescent measures taken on the external surface of the mouse, which suggests the feasibility of bioluminescence tomography for biomedical research using the small animals, especially the mice.

Keywords: Bioluminescence tomography (BLT), tissue phantom, optic fiber, light transmission, perturbation analysis.

1. INTRODUCTION

The translucency of the turbid tissue medium has facilitated investigations on biological tissues by optical means. The non-ionizing nature of the visible region of the spectral radiation further favors various techniques of optical imaging, such as continuous wave steady state, intensity modulated frequency domain, pulsed time-resolved, optical coherence, fluorescence and opto-acoustic methods[1]. Following these, bioluminescent imaging has been made possible due to the recent triumphs of molecular biology and the improved sensitivity of the cooled CCD system. Since the emission is due to the chemical reaction without any background influence, bioluminescent imaging has attracted more and more attention[2, 3]. The generated photons propagate from the luminescent sites to the surface of the animal. While photons are quite diffusive and become rather weak at their final destination, they serve as important information providers to depict neoplastic, dysplastic states of tissue and tumor metastasis[4]. In many cases, bioluminescent imaging is considered more sensitive than other imaging techniques[5].

Phantom experiments are required to analyze the photon propagation in various media and structures for developing bioluminescence tomography. Depending upon the tissue composition, structure and function, various organs such as the lungs, heart, kidney, brain *etc*. have different tissue optical properties[6, 7], including the absorption coefficient, scattering coefficients and anisotropy parameter. Different kinds of phantoms were developed using aqueous solutions with dyes, wax, resin, gel *etc*., and exploited for evaluating the performance of the imaging systems to observe the influence of abnormalities in control tissue models[8-12].

In this paper, we characterize the homogeneous physical phantoms whose optical properties are comparable with that of the lung tissue. To estimate optical parameters of the phantoms, experimentally measured reflectance or transmission

* Corresponding author: ge-wang@uiowa.edu

Developments in X-Ray Tomography IV, edited by Ulrich Bonse, Proc. of SPIE Vol. 5535
(SPIE, Bellingham, WA, 2004) · 0277-786X/04/$15 · doi: 10.1117/12.560530

flux is compared with theoretical predictions based on diffusion theory or Monte Carlo simulation[13]. Also, we report a perturbation analysis that examines the influence of intensity and displacement of a single source, as well as the effect of various separations of paired sources.

2. MATERIALS AND METHODS

2.1 Camera calibration

A system was developed in our laboratory for absolute light intensity calibration and sensitivity measurement of the nitrogen cooled CCD camera. The system consists of a calibrated tungsten light source (LS-1-Cal, Ocean Optics), a linear variable filter (LVF-HL, Ocean Optics), a light attenuator (FVA-UV, Ocean Optics), a bifurcated optic fiber (ZFQ, Ocean Optics) and a spectrometer (USB-2000 FLG, Ocean Optics). The schematic is shown in Fig. 1.

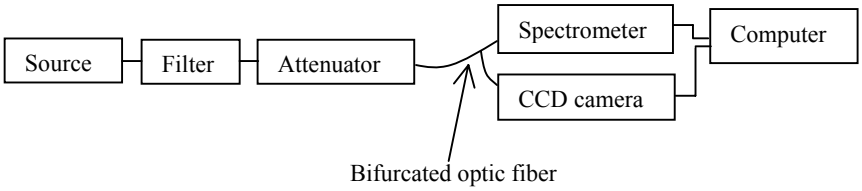

Fig. 1. Schematic of the system for intensity calibration and sensitivity measurement of the nitrogen cooled CCD camera.

The camera calibration was done for f-number f/2.8 and magnification 1x. The fiber was kept in front of the camera at a distance of 15cm away from the objective lens of the camera. The peak wavelength (λ = 650nm) with FWHM 25nm and arbitrary flux density was selected (OOIIrrad, Ocean Optics). The camera shutter was opened for 0.01second to obtain the image of the illuminating fiber surface of core diameter 50micron, and the corresponding maximum pixel value was noted. The average of 10 such observations was considered as the pixel gray level for the chosen flux density ($\pm 2.9\times10^{-17}$joules/count), and the same was repeated for various values. The flux density was converted into the number of photons entering into one pixel (20micron) of the CCD camera in one second. The best fit between flux density and pixel gray values was obtained by the following linear regression ($R^2 = 0.98$) equation:

$$\text{Flux density} = 8\times10^{-11}\times\text{pixel graylevel} \quad \text{Watts/cm}^2$$

As a result, the pixel values can be associated with the total flux density or number of photons. The sensitivity of the CCD camera was observed to be 13 photons/pixel-second.

2.2 Parameter estimation

Photons through the optic fiber from the source entered the cylindrical tissue phantom (white nylon) of diameter 20mm and height 30mm, as shown in Fig. 2. The CCD camera collected the transmitted light. To avoid the reentry of light due to the scattering from the sides of the phantom, it was coated with black.

The Monte Carlo simulation experiments were done using the TracePro software (Lambda Research Corporation, Littleton, US). It took as input the absorption and scattering coefficients as well as anisotropy parameter. The various transmission profiles were obtained with different combinations of these optical parameters. Using the trial and error method, the simulated and experimental plots were optimally matched. The optical parameters yielding the best-match ($\chi^2_{0.98}$) were assigned to the corresponding physical phantom[7, 11, 13].

2.3 Perturbation analysis

A rectangular slab (50mm×70mm×20mm) of the tissue phantom was fabricated for a perturbation study. Light guided through the optic fiber (core diameter 200μm) was delivered on the slab, and went upon the CCD camera for a short exposure time. The gray level in the image of the illuminating fiber was converted into flux density using the above-mentioned calibration formula. The following targets were perturbed, respectively.

For a single source with various incident flux densities of small differences, the CCD camera captured the corresponding transmitted signals. Then, the CCD camera took the outward light from the slab after displacing the source horizontally step-by-step away from the initial reference position with a given source intensity. Furthermore, the CCD camera recorded the light signals through two fibers of initial separation of 0.8mm with different fixed intensities, and repeated the measurement for different separation distances between these two optic fibers.

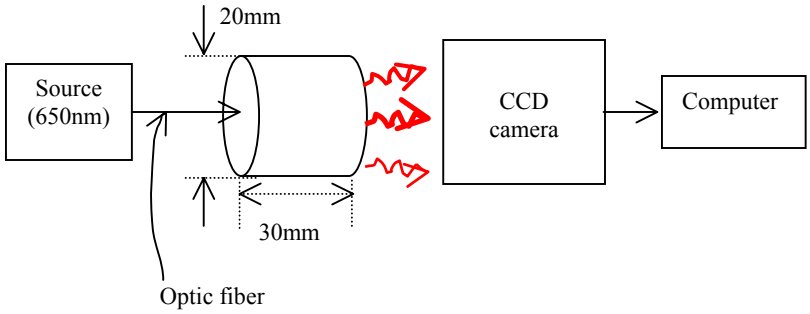

Fig 2. Schematic of the experimental system to obtain the transmitted signal through the phantom for estimation of its optical parameters.

Perturbation studies were also performed using heterogeneous phantoms with a single source of various flux densities of small differences and two sources of varying separation. The heterogeneous phantom was obtained by keeping two cylindrical phantoms attached to each other having same diameter (30mm) but with different heights viz. 25mm and 5mm whose optical parameters μ_a, μ_s, and g are 0.1mm^{-1}, 3.0mm^{-1} and 0.8 as well as 0.20mm^{-1}, 0.28mm^{-1} and 0.99, respectively.

The above settings were intended to mimic the presence bioluminescent source(s) with various intensities and separations inside the lungs of a small animal. Then, student's t-tests were applied to those data for quantification of the system sensitivity with respect to source intensity, position and/or separation.

3. RESULTS

Fig. 3 shows the experimental transmission profile of the tissue phantom and the best-matched simulation counterpart, which is associated with μ_a = 0.1mm^{-1}, μ_s = 3.0mm^{-1} and g=0.80. The reported scattering and absorption parameters of biological tissues vary widely, in the ranges of 1-300cm^{-1} and 0.1-10cm^{-1}, respectively. Accordingly, optical parameters of the nylon material, from which our lung tissue phantoms were made, were adjusted to the above regions[1, 6,13].

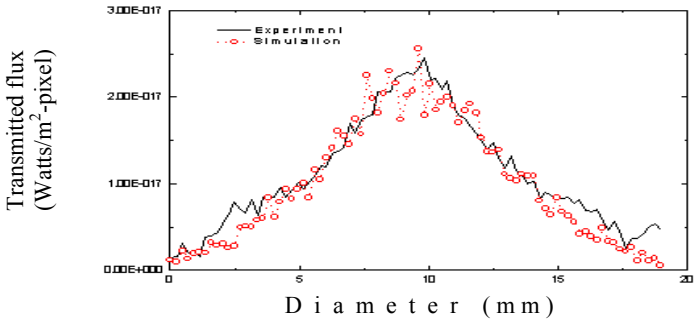

Fig 3. Transmission profiles curve for a cylindrical tissue phantom (white nylon) and the theoretically best-fit curve by Tracepro with g = 0.80, μ_a = 0.10cm^{-1} and μ_s = 3.0cm^{-1}.

Fig. 4 represents the transmission plots for the physical phantom with various incident source flux densities (1.91, 2.39 and 3.14nW/cm^2) and the corresponding simulation curves obtained using TracePro. It is observed that the transmission signal increases with increment of the source intensity. A significant difference in transmission corresponds to a minimum increment in source intensity of 0.5nW/cm^2. The significant change ($2p<0.05$) due to an increment in source intensity of 0.5nW/cm^2 indicates that about 40 photons would be needed for the detectability after the signal transmission through the phantom. This is not much worse relative to the sensitivity (about 13 photons) of the CCD camera itself (*i.e.*, exposing it directly to the source).

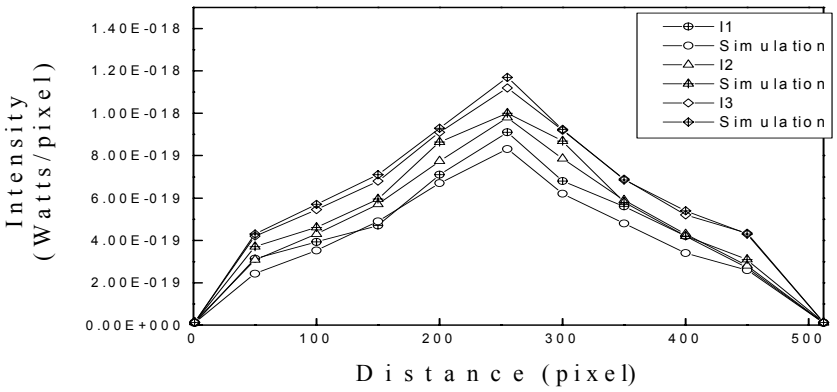

Fig 4. Transmission profiles for the physical phantom with incident source flux densities of 1.91 (I1), 2.39 (I2*) and 3.14nW/cm^2 (I3*) and their corresponding simulation profiles by TracePro (* $2p<0.05$ –Obtained by comparison of I2 and I3 with I1)

Fig. 5 presents the physically measured transmission profiles associated with one source of constant intensity that shifts horizontally in a small step 0.2mm for each measurement. The peak of the measured profile shows a clear shift along with the source movement. Our data reveal that the imaging system is capable of distinguishing a source displacement larger than 0.2mm, which happens to be the core diameter of the optic fiber.

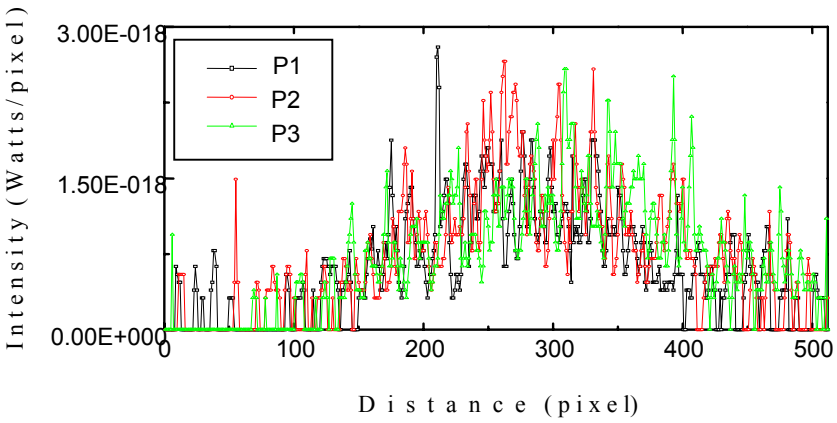

Fig 5. Transmission profiles from a physical phantom for incident source flux density of 3.4nW/cm^2 (±0.3nW/cm^2) at various positions P1 (reference position), P2* (P2=P1+0.2mm), and P3♠ (P3=P2+0.2mm) (* and ♠$2p<0.05$ obtained by comparison of P1 with P2 and P3 respectively).

In addition to the single source, the combined effect due to paired sources is illustrated in Fig. 6. Transmission profiles were obtained with two sources of separation 0.8mm (D1), 1.00mm (D2), 1.4mm (D3), 1.6mm (D4) and 2.0mm (D5). The source powers are 8.0±0.5 and 4.0±0.5nW/cm^2 for the bright source on the left and the weak one on the right respectively, as shown in Fig. 6(a). Comparisons among the measured profiles were made with that corresponding to D1 as the reference, as shown in Fig. 6(b). It is observed that by increasing the horizontal separation between the two sources, the flux decreases in the left portion of the panel, and the larger data points move to the right. The comparisons D1 vs. D5 and D1 vs. D3 indicate that the imaging system can detect a source-separation of about 2mm, albeit a bit conservatively.

Similar simulation experiments were also performed using the heterogeneous phantoms as given in table 1(a&b). First, the transmission profiles through the phantom were calculated with source intensity values 10, 11 and 12pW/mm^2, respectively. The significance in transmission was obtained with the change in flux of 2pW/mm^2. The next was to calculate the transmission profiles with two sources separated by various distances. Their separation ranges were from 0.3mm to 3.4mm with a 0.2mm increment. Two sources were set to have the same flux (1.0pW/mm2). The significance in transmission was obtained for the separation of 3.4mm. These may be attributed to the scattering characteristic of the medium. Further work is in progress to develop more tissue phantoms of various optical parameters for more detailed analysis.

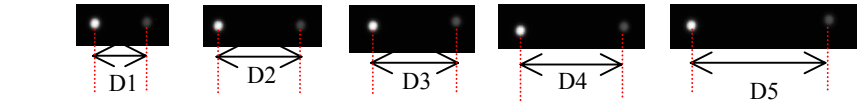

(a)

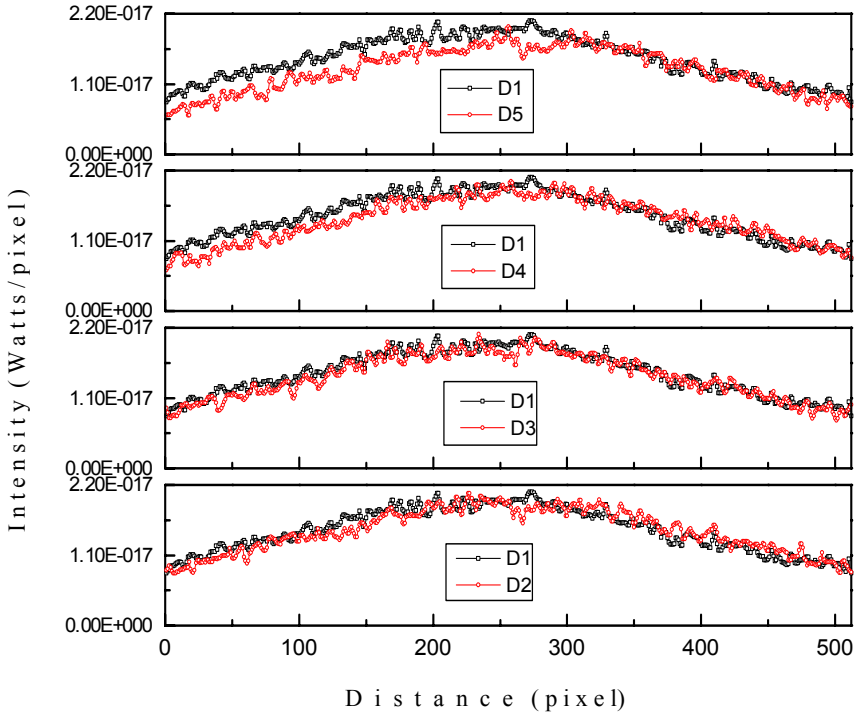

(b)

Fig 6. Perturbation analysis on detectability of separation of paired sources (a) Various separation of paired sources. (b) and corresponding transmission profiles through the physical phantom (* and $^\spadesuit$-2p<0.05 obtained by comparison of D1 with D4 and D5 respectively).

Table 1a. Diffused flux at the radial distance of 3mm from the cylindrical axis for different source irradiation. (student's t-test is carried out by comparing the diffused flux at the radial distance of 3mm for various source irradiation with the source irradiation of 10pW/mm^2)

Source Irradiation (pW/mm^2)	Diffused flux (x10^{-9} pW/mm^2)
10	2.68
	2.21
	2.58
	2.35
11	2.95
	2.43
	2.84
	2.58
12†	3.22
	2.65
	3.10
	2.82

† -2p<0.05.

Table 1b. Diffused flux at the radial distance of 3mm from the cylindrical axis for various sources separartion. (student's t-test is carried out by comparing the diffused flux at the radial distance of 3mm for various source separation with the sources separation of 0.30mm)

Sources separation (mm)	Diffused flux (x10^{-10} pW/mm^2)
0.30	9.18
	8.79
	7.39-21
	10.70
3.2	8.28
	7.64
	8.03
	9.17
3.4†	7.38
	6.67
	6.03
	7.14

† -2p<0.05.

4. CONCLUSION

In conclusion, the physical phantoms have been developed whose optical properties are comparable with that of the lung tissue. The perturbation analysis has revealed that changes in source intensity of 0.5nW/mm^2 or source shift of 0.2mm are needed to observe the significant difference in transmission data. As far as two point sources are concerned, a separation of 2-3mm is needed to distinguish the two sources directly based on a transmission profile. Our results have demonstrated that there is definite tomographic information inherent in bioluminescent data, which ought to be fully extracted for bioluminescence tomography.

Acknowledgment
This work is partially supported by the NIH/NIBIB grant 1R21EB001685.

REFERENCES

1. Valery Tuchin, *Tissue Optics: Light scattering methods and instruments for medical diagnosis*, SPIE Press, Berlingham, Washington, 2000.
2. T. F. Budinger, D. A. Benaron and A. P. Koretsky, "Imaging Transgenic Animals", *Annu. Rev. Biomed. Eng*., **1** 611-648, 1999.
3. S. R. Cherry, "In vivo molecular and genomic imaging: new challenges for imaging physics", *Phys. in Med. and Biol.*, **49**, 13-48, 2004.
4. B. W. Rice, M. D. Cable and M. B. Nelson, "In vivo imaging of light-emitting probes", *J. of Biomedical Optics*, **6**, 432-440, 2001.
5. Pritha Ray, Anna M. Wu and Sanjiv S. Gambhir, "Optical Bioluminescence and Positron Emission Tomography Imaging of Novel Fusion reporter Gene in Tumor Xenografts of Living Mice", *Cancer Research*, **63**, 1160-1165, 2003.
6. W. F. Cheong, S. A. Prahl and A. J. Welch, "A review of the optical properties of biological tissues", *IEEE J. Quant.Electr*., **26**, 2166-2184, 1990.
7. D. Kumar and M. Singh, "Characterization and imaging of compositional variation in tissues", *IEEE Trans. on Biomed. Eng*., **50**, 1012-1019, 2003.
8. M. Keijzer, W. M. Star and P. R. M. Storchi, "Optical diffusion in layered media." *Appl. Opt.*, **27**, 1820-24, 1988.
9. J .M. Schmitt, G. X. Zhou, E. C. Walker and R. T. Wall, "Multilayer model of photon diffusion in skin". *J. Opt. Soc. Am.*, **7**, 2141-2153, 1990.
10. Guillermo Marquez, Lihong V Wang, Changjie Wang and Zhibing Hu, "Development of tissue-simulating optical phantoms: poly-*N*-isopropylacrylamide solution entrapped inside a hydrogel", *Phys. in Med. and Biol.*, **44**, 309-318, 1999.
11. R. Srinivasan and M. Singh, "Laser Backscattering and Transillumination Imaging of Human Tissues and their Equivalent Phantoms", *IEEE Trans. on Biomed. Eng*., **50**, 724-730, 2003.
12. R. Cubeddu, A. Pifferi, P. Taroni, A. Toricelli and G. Valentini, "A solid tissue phantom for photon migration studies", *Phys. Med. Biol.* **42**, 1971-1979, 1997.
13. A.J. Welch and M. J. C. van Gemert, *Optical-Thermal Response of Laser-IrradiatedTissue*, Plenum Press, New York, 1995.